Research Article

Yong Wang*, Lizheng Zhang, Mingkun Qi, Zihan Yuan, Mingwei Li*, Wei Wang, Changlong Li, and Malik Yonis Hassan Saty*

Highly stretchable, durable, and reversibly thermochromic wrapped yarns induced by Joule heating: With an emphasis on parametric study of elastane drafts

https://doi.org/10.1515/epoly-2023-0189 received December 10, 2023; accepted January 11, 2024

Abstract: Highly stretchable thermochromic wrapped yarns, which employ elastane filament (EF) as core, stainless steel wire, and thermochromic polyester filament as the first and second winding, was prepared, and the effect of elastane draft upon yarn properties was investigated. It was found that the elastane draft played an essential role in determining the final yarn behavior, and the optimized elastane draft parameter was 2.5 using Technique for Order Preference by Similarity to Ideal Solution. It is a distinctive configuration of yarn's constituents and the EF draft that are responsible for the exceptional stretchability of yarns, and it showed mechanical robustness following cyclic stretch. Importantly, the yarn exhibited rapid, durable, and reversible color conversion when subjected to cyclic voltage, cyclic abrasion, and alkali. Finally, a flower-shaped pattern was fabricated by

embroidering yarn onto an elastic substrate as a proof-ofconcept, and no obvious variation of color fidelity was observed during the stretch.

Keywords: elastic thermochromic yarn, hollow-spindle wrap spinning, draw ratio, metal wire, Joule heating

1 Introduction

We have witnessed the rapid development in the fabrication of functional and/or smart materials with the rise of functional and/or smart textile concepts (1-6). Smart textiles with tunable color-changing performances, an important branch of smart materials, have attracted growing attention in recent years mainly due to their extensive potential uses in colored display, sensing, anti-counterfeiting, and military camouflage (7). As the basic building blocks of smart color-changing textiles, smart fibers and/or yarns with excellent flexibility/stretchability, implantability, and adaptability become the focus of much research and are urgently needed (8). However, the colors of existing commercial fibers and/or yarns cannot be changed on demand due to the passive optical behaviors of traditional dyes. As a consequence, it is imperative to conduct a thorough investigation of principles involved in rational selection and structural configuration of constituents in these fibers and/or yarns in a penetrating way.

Substantial information, available in the literature, has been given about the fabrication procedures of smart color-changing materials in fiber- (8–19), yarn- (20–23), and fabric-forms (24–28). Prior to the present study, for instance, at the fiber scale, Fan et al. prepared stretchable electrother-mochromic fibers using elastic conductive fibers with hierarchical porous structures as the core layer and thermochromic coatings as the shell layer (9). Li et al. proposed a method to fabricate electrochromic fibers based on a helically twined

Lizheng Zhang, Mingkun Qi, Zihan Yuan, Changlong Li: Advanced Fiber Materials Engineering Research Center of Anhui Province, College of Textiles and Garments, Anhui Polytechnic University, Wuhu, 241000, China

Wei Wang: College of Chemistry and Chemical Engineering, Donghua University, Shanghai, 201620, China

^{*} Corresponding author: Yong Wang, Advanced Fiber Materials Engineering Research Center of Anhui Province, College of Textiles and Garments, Anhui Polytechnic University, Wuhu, 241000, China; Key Laboratory of Clean Dyeing and Finishing Technology of Zhejiang Province, Shaoxing, 312000, China; National Local Joint Laboratory for Advanced Textile Processing and Clean Production, Wuhan, 430200, China, e-mail: wangyong@ahpu.edu.cn

^{*} Corresponding author: Mingwei Li, Wuhu Fiber Inspection Institute, Wuhu, 241000, China, e-mail: 1007609345@qq.com

^{*} Corresponding author: Malik Yonis Hassan Saty, Advanced Fiber Materials Engineering Research Center of Anhui Province, College of Textiles and Garments, Anhui Polytechnic University, Wuhu, 241000, China; College of Engineering Technology of Industries, Sudan University of Science and Technology, Khartoum, 11111, Sudan, e-mail: malik.saty@hotmail.com

metal electrode structure using three types of conjugated polymers, and multiple color-changing effect can be obtained (10). However, the as-prepared fibers cannot be macroscopically stretched. Li et al. prepared a flexible and stretchable stripshaped thermochromic resistive heater textile by paving CNT sheets on a pre-stretched thermochromic silicone elastomer, and it has a rapid thermal response and excellent stability following cyclic stretch (11). Ran et al. proposed a method combining impregnation and electrospinning to fabricate CNT/PU core-sheath nanocomposite fibers. The fibers exhibited straindependent conductivity, and electrothermochromic properties (12). Sin et al. proposed a straightforward method to fabricate stretchable thermo- and mechanochromic fiber with a liquid metal core. The hollow stretchable fiber was prepared using silicone composite with thermochromic pigments, and then, the liquid metal was injected into the hollow fiber core. The colorchanging effect can be triggered by applying Joule heating through the liquid metal (19). A minor review demonstrating that the fibers above may involve complex preparation process, and the large-scale production may be limited.

At the yarn scale, Yang fabricated electrothermochromic yarn by wrapping pure cotton yarn on CNT/cotton composite yarn, followed by coating with thermochromic inks (20). Although multiple color-changing effects can be obtained, the as-prepared yarn cannot be stretched, and the adhesive stability of inks on the yarn surface may not be strong enough. Pan et al. pointed out that the core-sheath electrothermochromic composite yarns can be prepared by electrospinning PU nanofibers containing different thermochromic inks onto CNT/cotton yarns. The CNTs inside provide reversible electrothermal behavior, and the PU layer helps maintain the yarn shape and provides a platform to load inks (21). Junge et al. prepared multi-layer hybrid yarns, which employ stainless steel wire (SSW) as the conductive core, polyester filament wrapped around the core as winding, and it serves as substrate medium for thermochromic material coating (23). A minor review revealed that the yarns mentioned earlier lack stretchability, which remarkably limited their steps in the realization of body-conformable wearable textiles.

At the fabric scale, Chen et al. stitched stainless steel conductive yarns on cotton fabrics, and then, fabrics were screen-printed with black thermochromic leuco dye pigment (24). The stretchability of such fabrics is not available, and durability was not involved. Jiang et al. introduced thermochromic microcapsules onto the surface of cellulose aerogel fiber fabric (25). Chowdhury et al. fabricated a conductive fabric using nichrome/cotton core-spun yarn as the weft and pure cotton as the wrap, and then, thermochromic pigments were coated onto the fabric surface (26). Huang et al. proposed a simple approach to prepare a smart color-changing textile based on commercially available polyester-

covered cotton fabric. The conductive substrate was produced by selective deposition of PPy on the cotton side of the above fabric, while the thermochromic ink was painted on the polyester side (28). A minor review revealed that the thermochromic fabrics above lack stretchability, and such fabrics can only work as a whole, which may not easily realize local heating and thermochromic effect.

As is evident from the aforementioned brief introduction, textile yarns as the intermediates between fibers and fabrics should be further developed to satisfy several requirements: first, the color of yarns should be easily controlled and precisely triggered on demand; second, the yarns should be macroscopically stretchable to realize body conformability and wearing comfortability during human body joint movement in an imperceptible way; third, facile fabrication procedure and large-scale production are highly needed for the practical uses of smart yarns; last, the yarns are expected to be easily integrated with multifunction such as local heating.

To achieve the above goals, herein, a facile fabrication procedure of highly stretchable and durable thermochromic wrapped yarns induced by Joule heating was proposed (see Figure 1), purposely avoiding the disadvantages of traditional textile dyeing procedure. The elastane filament (EF) located in the center offers the controllable stretchability of wrapped yarns, the first layer of SSW was used as a heatconducting material and can generate Joule heat by controlling the voltage precisely, and the color of the second layer of thermochromic polyester filament (TCPF) can be converted when the heat reaches its threshold temperature. The effect of elastane draft on tensile and elastic properties of yarns was investigated systematically, and the optimized elastane draft was determined using Technique for Order Preference by Similarity to Ideal Solution (TOPSIS). Finally, a stretchable dynamic colored display based on as-prepared yarn was demonstrated.

2 Experimental

2.1 Raw materials and basic tensile behaviors

Herein, three raw materials of EF (1120 D), SSW (with a diameter of 35 μ m), and TCPF (75 D×2, the color switched from purple to pink with a threshold temperature above 30°C) were used to fabricate highly elastic thermochromic wrapped yarns. The surface structures of raw materials were examined using optical microscopy, and the results

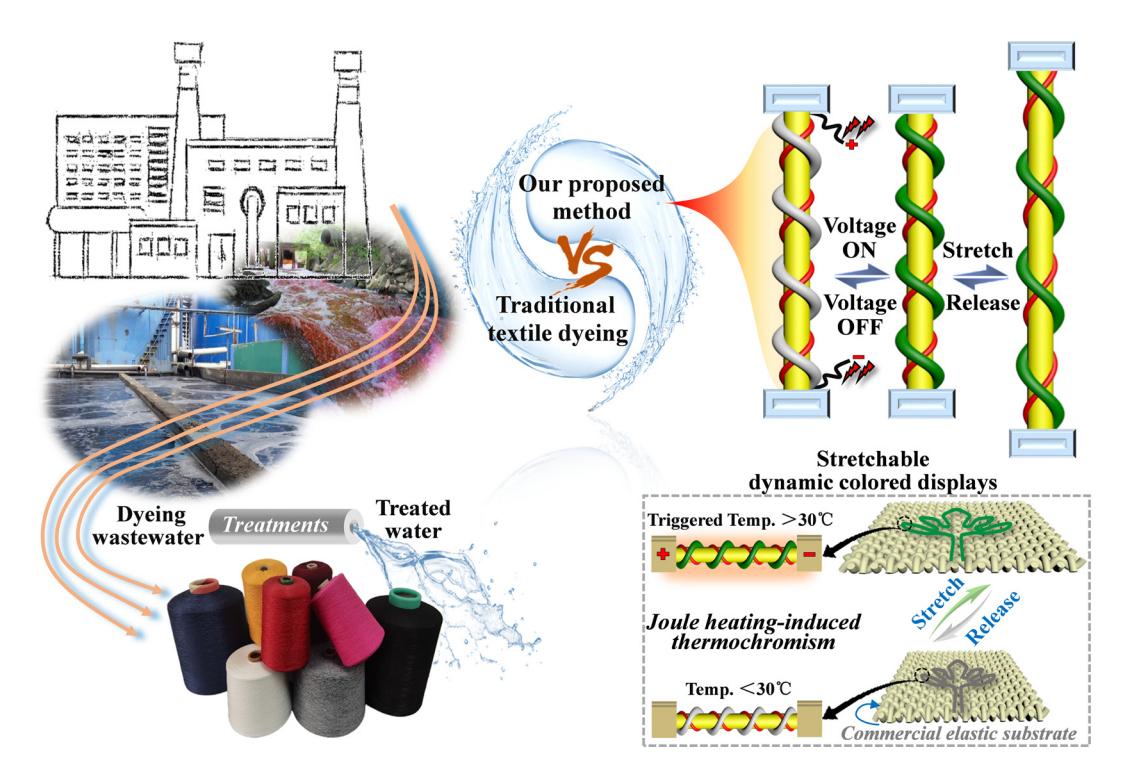


Figure 1: Fabrication of elastic thermochromic wrapped yarns enabling stretchable dynamic colored displays, purposely avoiding the disadvantages of traditional textile dyeing.

are shown in Figure 2a–c, respectively. It can be visibly seen that the three materials behave mechanically totally differently.

2.2 Preparation of elastic thermochromic yarns with varying elastane drafts

The stretchable thermochromic wrapped yarns were fabricated using a hollow-spindle wrap spinning frame, as graphically illustrated in Figure 3a. As can be visibly seen, the EF core was fed through the positive feed rollers and located in the center of the lower hollow tube, the SSW wrapped on the surface of a lower hollow spindle was

unwound and jointed with the EF core, forming a combination. Then, the TCPF wrapped on the higher hollow spindle was unwound and joined with the preformed combination mentioned earlier. Finally, the elastic thermochromic-wrapped yarns were created.

The spinning technological parameters play a vital role in influencing the yarn structure and hence, the final properties. Based on some preliminary trials, the predetermined elastane draft of EF was regulated from 1.5 to 4.0 (i.e., 1.5, 2.0, 2.5, 3.0, 3.5, and 4.0), and some other parameters were summarized as follows: wrapping density 800 T·m⁻¹, outer-inner twist ratio 1.0, and spindle speed 5,000 rpm. Note that, all the yarn samples were fabricated on the same spinning head

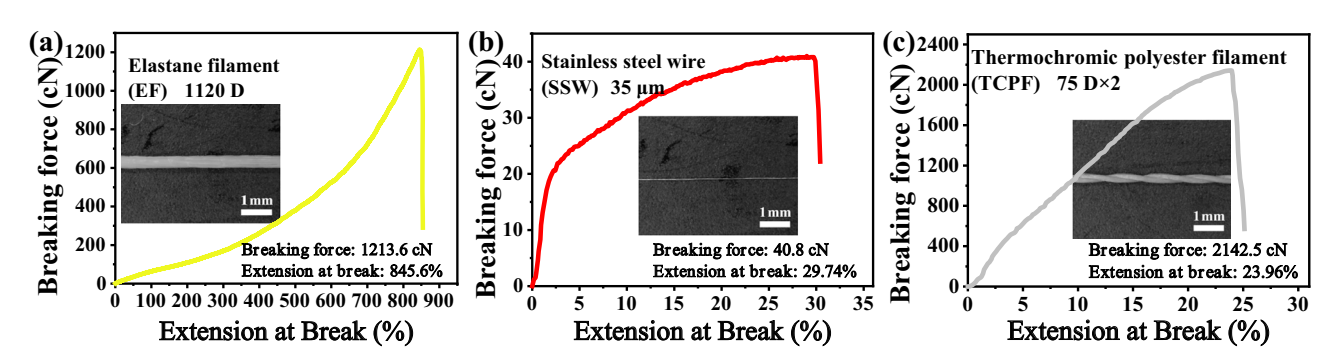


Figure 2: Typical tensile curves and surface structures of (a) EF, (b) SSW, and (c) TCPF, respectively.

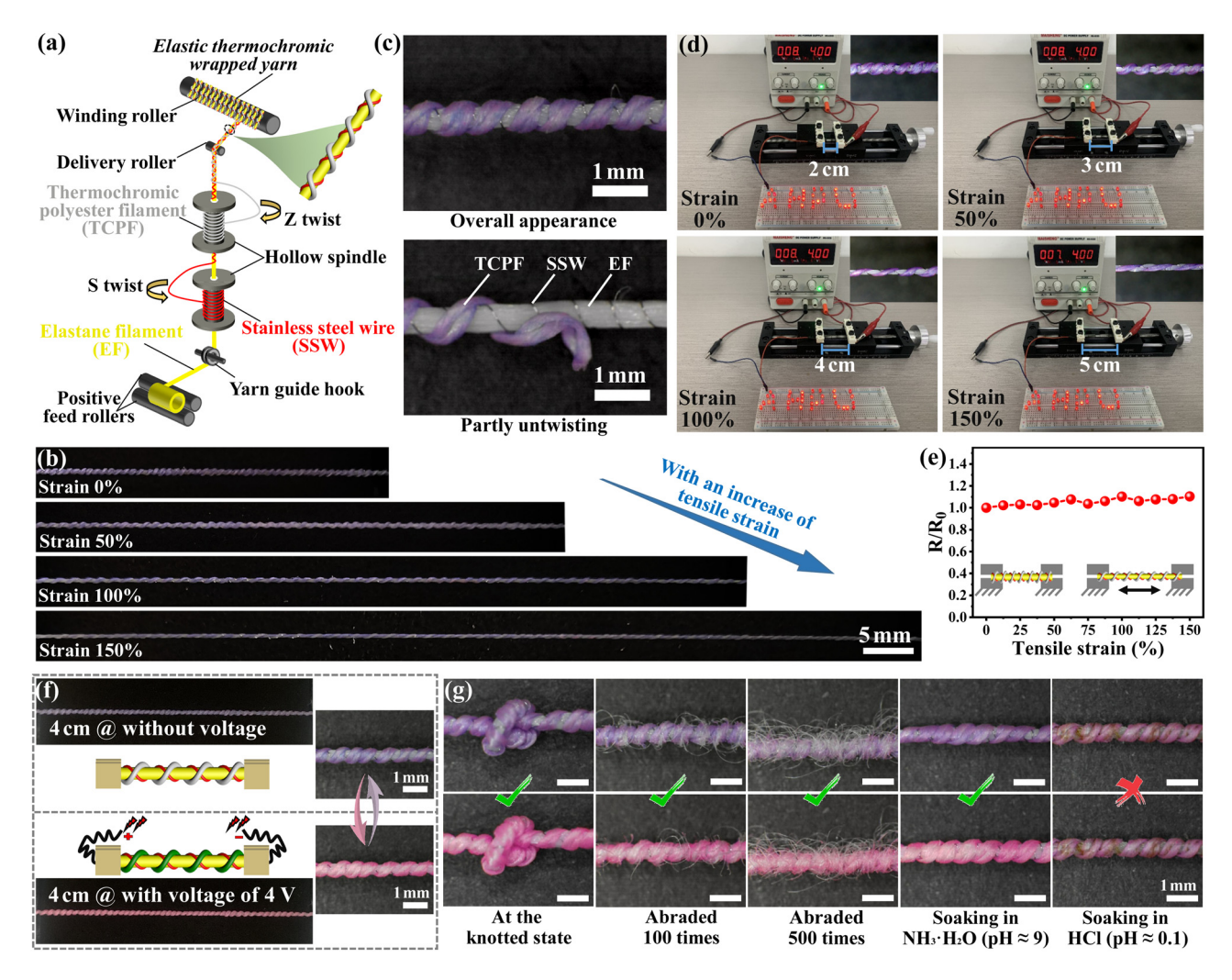


Figure 3: (a) Schematic diagram of fabrication procedure of elastic thermochromic wrapped yarns; (b) macroscopic stretchability of yarn spun with elastane draft of 2.5; (c) microscopic structure of the yarn; (d) yarn was used as a stretchable conductor to power the "AHPU" logo at different strains at 4 V; (e) stable conductivity of yarn sample during the stretching process; (f) characterization of Joule heating-induced thermochromism of yarn; and (g) thermochromic durability of yarn.

with the predefined conditions, in order to minimize variations during the whole spinning process.

Figure 3b displays the stretching process of a wrapped yarn sample spun with elastane draft of 2.5. The yarn has a more bulking surface profile compared with the extended one, which facilitates its elasticity up to an extremely high strain of about 150% without distortion. No macroscopically obvious structural change of yarn takes place following 10 cyclic tests. Additionally, we have also observed that the resultant yarns spun with elastane draft of 1.5 and 4.0 can be extended to 50% and 300% strain, respectively. To sum up, it is the distinctive configuration of yarn's constituents (SSW and TCPF) and the draft applied to EF that are mainly responsible for the exceptional stretchability of as-prepared wrapped yarns. Figure 3c gives the microscopic yarn structure. Three components can be visibly

seen; the EF served as the core and was tightly wrapped by SSW in one direction and TCPF in an opposite direction.

As presented in Figure 3d, owing to the excellent electrical conductivity of the as-prepared yarn, it can be used as a flexible conductor to light the "AHPU" LED logo at 4 V. More importantly, the "AHPU" logo keeps high brightness even though the yarn was 150% stretched, indicating the stable conductive reliability (Figure 3e) with high flexibility and elasticity of as-fabricated yarn during stretch.

Further, based on some preliminary trials, for a yarn with an initial length of 4 cm, a voltage beyond 3 V can generate a temperature higher than the threshold temperature of TCPF within a yarn. Herein, a voltage of 4 V was applied to two ends of yarn with 4 cm length, as presented in Figure 3f. The color of the yarn converts from purple to pink within only a few seconds (<2 s). It can be

reversibly controlled color change by turning on and off voltage without an observable loss of fidelity. The heat originating from the thermal resistance effect of SSW inside in conducting electricity is responsible for triggering the thermochromism of the varn. In addition, as shown in Figure 3g, the yarn showed color change even at a knotted state. It exhibited excellent thermochromic durability subjected to cyclic abrasion (e.g., 100 and 500 times), although yarn hairiness gradually increases with increasing abrasion numbers. The chemical resistance was also evaluated by soaking the varn into acid (pH \approx 0.1)/alkali (pH \approx 9.0) solutions and stirring at a speed of 40 rpm for 15 min. It was found that the color-changing was immune to alkalis, but strong acids had adverse effects.

2.3 Characterization

All the yarn samples were conditioned at in ambient temperature of 20 \pm 2°C and relative humidity of 65 \pm 3% for at least 24 h before testing.

2.3.1 Tensile behavior

2.3.1.1 Tensile fracture

Tensile behavior of yarns was measured using a YG(B) 021DL tensile tester. Each sample was tested 40 times at a gauge length of 50 mm and a pretension of 0.5 cN·tex⁻¹ with a speed of 500 mm·min⁻¹ according to China standard GB/T 3916-2013 and FZ/T 12034-2012. Fracture modes, that is, drastic fracture (simultaneous fracture) and non-simultaneous fracture for each sample were recorded. Moreover, box-whisker plots were used to characterize the tensile force of yarns with different draw ratios.

2.3.1.2 Cyclic tensile tests at varying strains

A yarn with the same test conditions was tested with a PT-1198GTD-C universal mechanical instrument to stretch it to the determined strains (50% and 100%), and then, the tension was unloaded to the initial position. Five cyclic tests were performed.

2.3.2 Elastic behavior

The elastic testing procedure of yarns is illustrated in Figure 5a. The initial yarn length of 25 cm was determined with a preload ($F_{\text{pre}} = (\text{Tex}_{\text{EF}}/D_{\text{EF}} + \text{Tex}_{\text{SSW}} + \text{Tex}_{\text{TCPF}}) \times 0.88 \text{ cN-tex}^{-1}$,

here, $D_{\rm EF}$ refers to the draw ratio of EF), and the position at the first stage was marked as OA. Then, 50% of the average breaking force of the yarn was determined as the applied load, and the load was applied to the yarn, held for 60 s, and the position at the second stage was marked as OB. After that, the yarn with preload was unloaded for 120 s relaxation, and the position at the third stage was marked as OC. Finally, two indices, that is, elastic extension ratio (ε) and elastic recovery ratio (R), can be calculated.

$$\varepsilon = \frac{OB - OA}{OA} \times 100\% \tag{1}$$

$$R = \frac{OB - OC}{OB - OA} \times 100\% \tag{2}$$

2.3.3 Surface morphology

The surface morphology for each yarn sample was determined using a USB microscope. It should be noted that the varn sample under different extensions was observed with the help of a screw guide system.

2.3.4 Color-changing and electrothermal behaviors

As for color-changing behavior, a varn sample of 12 cm in length with an optimized draw ratio was embroidered onto an elastic textile substrate, forming a flower-shaped pattern. Then, the positive and negative poles of a power supply (MS-605D) were clamped to the yarn's SSW ends, and a voltage of 12 V was applied. Finally, color variations of the pattern were recorded using a digital camera to characterize color-changing behavior under different testing conditions, e.g., initial state, different amounts of stretch.

Moreover, the electrothermal behavior of the above pattern with different voltages was monitored using a FLIR E5XT thermal imager. In addition, the pattern was stretched from 0% to 50% strain, respectively, and the temperature variation and color change were recorded using the thermal imager and a digital camera, respectively.

3 Results and discussion

3.1 Effect of elastane draft on tensile behavior of yarns

Figure 4a highlights the upward trend of breaking forces of wrapped yarns as a function of increasing elastane drafts

6 — Yong Wang et al. DE GRUYTER

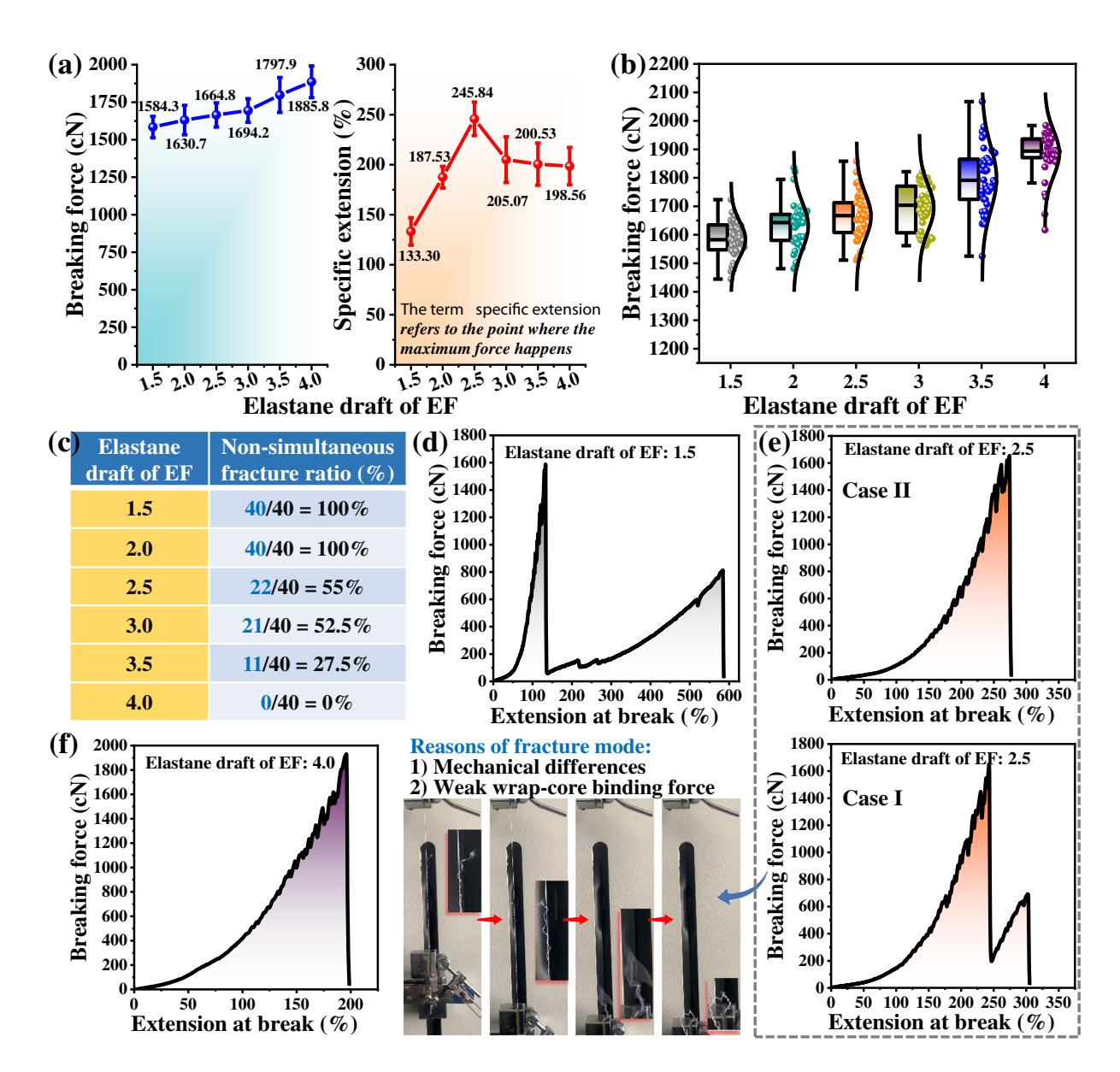


Figure 4: (a) Effect of elastane draft on the tensile response of the resultant wrapped yarns; (b) Box-whisker plots of breaking force of yarns; (c) the non-simultaneous fracture ratios of wrapped yarns with varying elastane drafts; (d)–(f) representative tensile curves of yarns with elastane drafts of 1.5, 2.5, and 4.0, respectively. Inset shows captured photographs of yarns during the stretching process.

on the whole. The primary reasons are explained as follows: first, with an initial increase in the draw ratio of core elastane, the proportion of wrapped components in the yarn cross-section increases. Consequently, there are more wrapped components taking up the load in wrapped yarn when elastane stretch increases initially. Since the breaking force of wrapped components (i.e., SSW and TCPF) are larger than that of elastane core within the range of breaking strain of wrapped components, as a result, a positive contribution to the final breaking strength of yarns was made. Second, compared with lower elastane drafts, the higher frictional contact with

individual fibers inside the yarn and the larger pre-extension of core elastane were found with the higher elastane drafts of EF, which in turn reduced the mechanical difference between the core EF and the sheath (i.e., SSW and TCPF). In that case, the yarn can withstand greater external force during stretch, making a positive contribution to the final tensile strength of yarns with elevated elastane drafts. Besides, the term "specific extension" refers to the point where the maximum force happens. As can be seen, the specific extension of yarns increased first to a maximum with increasing elastane drafts up to 2.5, beyond which it reduced drastically. The relevant results in

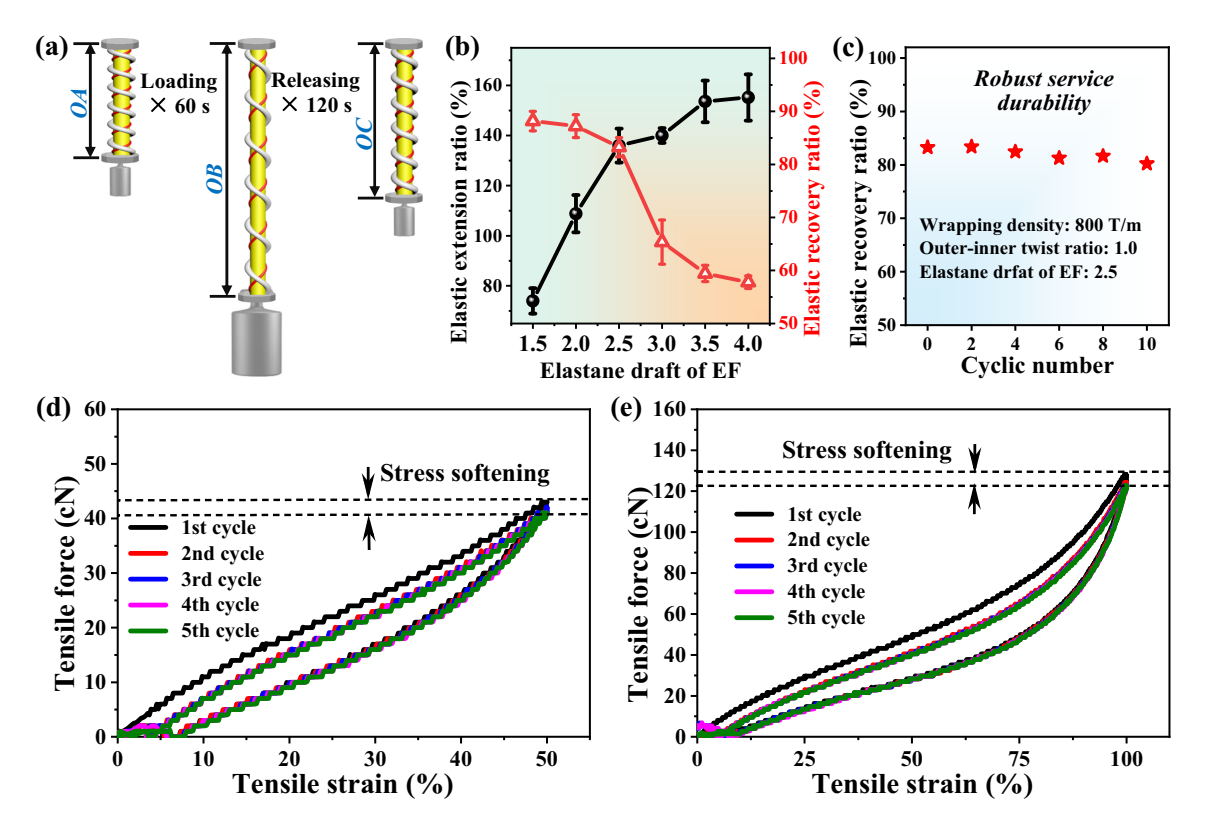


Figure 5: (a) Schematic diagram of elastic testing procedure of wrapped yarns; (b) effect of elastane draft on elastic properties of the resultant wrapped yarns; (c) elastic recovery ratio of a yarn sample following cyclic tests; (d)–(e) cyclic tensile behaviors of yarn sample at a tensile strain of 50% and 100% following five cyclic tests, respectively.

Figure 4a are reflected in Figure 4b, which presented the median and quartile breaking force values of wrapped yarns with elevated elastane drafts. The box-whisker plot is a simple but powerful analytical tool that can reveal more visual information about the underlying characteristics of a tensile distribution. As seen, as the elastane drafts of EF increased, the median gradually increased. With consideration of the shape of the tensile distribution, the box-whisker plots for most groups are obviously negatively/left skewed.

Further, because of the sophisticated structure of our yarns, the fracture modes behave totally differently. As shown in Figure 4c, a decreased variation of non-simultaneous fracture ratio of yarns with elevated elastane drafts of EF can be found. For example, 100% non-simultaneous breakage at elastane drafts of 1.5 and 2.0 was found, and the ratio reduced to 55%, 52.5%, 27.5%, and 0% at elastane drafts of 2.5, 3.0, 3.5, and 4.0, respectively. The results were also reflected in Figure 4d–f. As shown in Figure 4d, the yarn presents a "two-phase" tensile failure (two peaks) and shows a larger breakage tail with sharp breaks. As shown in Figure 4e, two kinds of breakage of yarn with an elastane draft of 2.5 can be found. One kind is sharp and drastic breakage, and another kind is "two-phase" failure mentioned above. It is the mechanical difference between the

wrap and core and the weak wrap-core binding force that are responsible for the "two-phase" failure mode of the resultant yarn (see the inset). As seen in Figure 4f, with a further increase of elastane draft, the yarn depicts a single and sharp breakage, suggesting that all the components within a yarn break simultaneously. In comparison, with an increase of elastane draft, the breaking points of the first breaking peak of wrapped yarns show a first rising and then declining variation trend, which contributes to the breakage conversion of yarns from non-simultaneous to simultaneous fracture.

3.2 Effect of elastane draft on elastic behavior of yarns

The schematic of the elastic testing procedure of as-prepared wrapped yarns is illustrated in Figure 5a, and the detailed results of yarns with different elastane drafts are presented in Figure 5b. As shown, an upward trend of the elastic extension ratio of the resultant yarns with different elastane drafts was highlighted, whereas a downward trend was seen for the elastic recovery ratio, which demonstrates the elastane draft is a key factor influencing yarn elastic behavior. As expected, a positive effect was made between the elastic extension ratio and elastane draft of the resultant yarns, which is mainly due to the fact that higher elastane stretch during the yarn spinning process results in more ability for varn extension, allowing the wrap components within a yarn to reach its ultimate extension. On the other hand, theoretically, the yarns have superior elastic resilience with an increase of elastane draft. However, the increase in elastane draft reduces elastic recovery. This may be due to the fact that as elastane draft increases, the wrap (i.e., SSW and TCPF) within a yarn in its initial state are tightly and firmly arranged with each other, the available mobility of the wrap reduces accordingly. Consequently, the effect of restraint takes place on the elastic recovery of yarns with elevated elastane drafts. Besides, the existent creeping effect of yarns with elevated elastane draft is detrimental to the elastic recovery property. In short, a negative effect was created between the elastic recovery ratio and the elastane draft of the as-prepared wrapped yarns.

As for an elastic textile yarn, structural stability, and elastic robustness are of importance for its practical uses. As shown in Figure 5c, taking a yarn sample with an elastane draft of 2.5 for example, no obvious deteriorated variation was found following 10 cyclic tests, indicating the robust service durability and excellent elasticity of our wrapped yarns. Figure 5d and e shows the cyclic tensile curves at strains of 50% and 100%, respectively. As can be seen, for any of the above-given strains, the shapes of all curves of yarn following different cycles and the areas of the corresponding hysteretic loops are almost the same, except for the first cycle. Moreover, the maximum force achieved at consecutive cycles marginally decreased, and the "stress softening" of yarn generated following cyclic tests is primarily responsible for the variation. Besides, only smaller residual strains were seen, irrespective of the strain considered, which reflects the structural and elastic robustness of as-prepared yarn even if it undergoes larger tensile extension.

3.3 Elastane draft optimization using TOPSIS

In this part, TOPSIS, a multi-criteria decision-making method, was used to optimize the elastane draft parameter of the resultant wrapped yarns. The TOPSIS method consists of the following steps:

Step I: Construct the decision matrix

Based on objective criteria, a decision matrix is constructed and expressed based on the response variables, as presented in Eq. 3.

$$X_{ij} = \begin{bmatrix} A_1 & X_{11} & X_{12} & X_{13} & \dots & X_{1n} \\ A_2 & X_{21} & X_{22} & X_{23} & \dots & X_{2n} \\ A_3 & X_{31} & X_{32} & X_{33} & \dots & X_{3n} \\ \dots & \dots & \dots & \dots & \dots & \dots \\ A_m & X_{m1} & X_{m2} & X_{m3} & \dots & X_{mn} \end{bmatrix}$$
(3)

where A_1 , A_2 , A_3 ,..., A_m are the possible alternatives among which decision-makers have to choose the best one. For i = 1 to m; j = 1 to n; x_{ij} represents the actual value of the ith experimental result for the jth process response.

Step II: Normalize the decision matrix

The decision matrix was normalized. The output values can be expressed as follows.

$$T_{ij} = \frac{X_{ij}}{\sqrt{\sum_{i=1}^{m} X_{ij}^2}} \tag{4}$$

where i = 1 to m; j = 1 to n; x_{ij} represents the actual value of the ith experimental result for the jth process response; and T_{ij} represents the corresponding normalized value.

Step III: Calculate the objective weight and the weighted matrix

The entropy weight method is proposed to assign and determine the different weights to different characteristics of yarns. Then, the weighted normalized decision matrix is calculated by multiplying the normalized matrix by its related entropy weights.

$$V_{ij} = W_i \times T_{ij} \tag{5}$$

where i = 1 to m; j = 1 to n; and W_j represents the entropy weight of jth attribute.

Step IV: Estimate the positive and negative ideal solution Herein, the positive (V^+) and negative (V^-) ideal solutions for the relative rankings of the parameters need to be determined before the priority of wrapped yarns with m types of parameters and n types of evaluation criteria can be ranked.

$$V^{+} = (V_{1}^{+}, V_{2}^{+}, V_{3}^{+} \dots V_{n}^{+}), \text{ where } V_{j}^{+} = \{\max(V_{ij})\}\$$

$$V^{-} = (V_{1}^{-}, V_{2}^{-}, V_{3}^{-} \dots V_{n}^{-}), \text{ where } V_{i}^{-} = \{\min(V_{ij})\}$$
(6)

where i = 1 to m; j = 1 to n; and W_j represents the entropy weight of jth attribute.

Then, the relative degree of separation between each experimental data and positive and negative ideal solutions can be calculated as follows:

$$S_{i}^{+} = \sqrt{\sum_{i=1}^{m} (V_{ij} - V_{j}^{+})^{2}}$$

$$S_{i}^{-} = \sqrt{\sum_{i=1}^{m} (V_{ij} - V_{j}^{-})^{2}}$$
(7)

where i = 1 to m; j = 1 to n.

 $\begin{tabular}{ll} \textbf{Step V}: Determination coefficient of closeness and \\ ranking order \end{tabular}$

The coefficient of closeness (CC) is calculated.

$$CC = \frac{S_i^-}{S_i^+ + S_i^-} (0 < CC < 1)$$
 (8)

Finally, the calculated results of CC are ranked and TOPSIS rankings were determined. A higher coefficient of closeness represents a favorable experimental run.

Based on the above description of the TOPSIS method, the elastane draft of wrapped yarns was optimized, and the detailed results are summarized in Tables 1 and 2.

Table 1 summarizes the relative entropy values of yarns with different elastane drafts. As seen, the elastic recovery ratio has the highest entropy weight value of 35.063%, whereas specific extension has the smallest value of 17.293%. The above results indicate that the elastic recovery behavior is an essential factor in influencing the final yarn behavior. Furthermore, there is a negative correlation between the information entropy value and the entropy weight. Besides, a complement relationship can be found between the information entropy value and the information utility value (e + d = 1).

Table 2 displays the separation matrix (S_i^+, S_i^-) and coefficient of closeness (CC) for each experiment. A high CC indicates that the experimental and ideal values are similar. As seen, the third group holds rank one with wrapped yarn with the optimized elastane draft of 2.5, whereas the elastane draft of 1.5 is viewed as the worst condition.

3.4 Stretchable dynamic colored displays

Herein, a yarn spun with the optimized elastane draft of 2.5 was used. The yarn can be industrially woven, knitted, embroidered, etc. Since embroidery allows for the pathway to be laid out in a more free-form fashion, the yarn can travel wherever needed over the textile surface so that yarn can be arranged in any direction through pattern designing. As a proof-of-concept, the yarn sample was processed into a flower-shaped pattern and embroidered onto the wrist guard's surface as a stretchable dynamic color

Table 2: Ranking of the optimized solution of yarns with varying elastane drafts

Elastane draft	Positive separation matrix (S_i^+)	Negative separation matrix (S_i^-)	Coefficient of closeness (CC)	Rank
1.5	0.80583306	0.59213730	0.4236	6
2.0	0.56522041	0.63920231	0.5307	3
2.5	0.42481109	0.73707630	0.6344	1
3.0	0.58995463	0.49806217	0.4578	5
3.5	0.60619685	0.61844517	0.5050	4
4.0	0.61737208	0.73115509	0.5422	2

display, aiming to show excellent color-changing effect during the stretch, as illustrated in Figure 6a.

In as-prepared thermochromic wrapped yarn, the Joule heating originates from the thermal resistance effect of the SSW component inside in conducting electricity. As seen in Figure 6b, the voltages applied were varied from 4 to 12 V, and the steady-state surface temperature was noted to increase with voltage. In order to trigger the thermochromism of the pattern, the minimum voltage required is about 6 V. In that case, the surface temperature is about 30.5°C, higher than the threshold temperature of the TCPF component inside the wrapped yarn. The captured thermal images of patterns at elevated voltages were also recorded. Besides, we have observed that the fully color-changing time of such a pattern is smaller when a higher voltage was applied, although the color can be switched at 6 V. Therefore, when a voltage of 12 V was applied, the color switched from purple to pink completely within 2s, indicating its rapid thermochromic response.

In practical use, maintaining a robust colored display of textiles during a stretch is of very importance. Since the expansion strain across different body parts during movement is between 20% and 70%, the thermochromic performance of the above flower-shaped pattern was measured at different amounts of stretch, as shown in Figure 6c. For a predetermined voltage of 12 V, with an increase of tensile strain, the saturated surface temperature of the pattern was noted to decrease, and the minimum surface temperature of 37.4°C was obtained when the pattern was subjected

Table 1: Summary of relative Entropy values of yarns with varying elastane drafts

Terms	Information entropy value (e)	Information utility value (d)	Entropy weight (%)
Breaking force	0.790	0.210	30.084
Specific extension	0.880	0.120	17.293
Elastic extension ratio	0.878	0.122	17.560
Elastic recovery ratio	0.756	0.244	35.063

10 — Yong Wang et al. DE GRUYTER

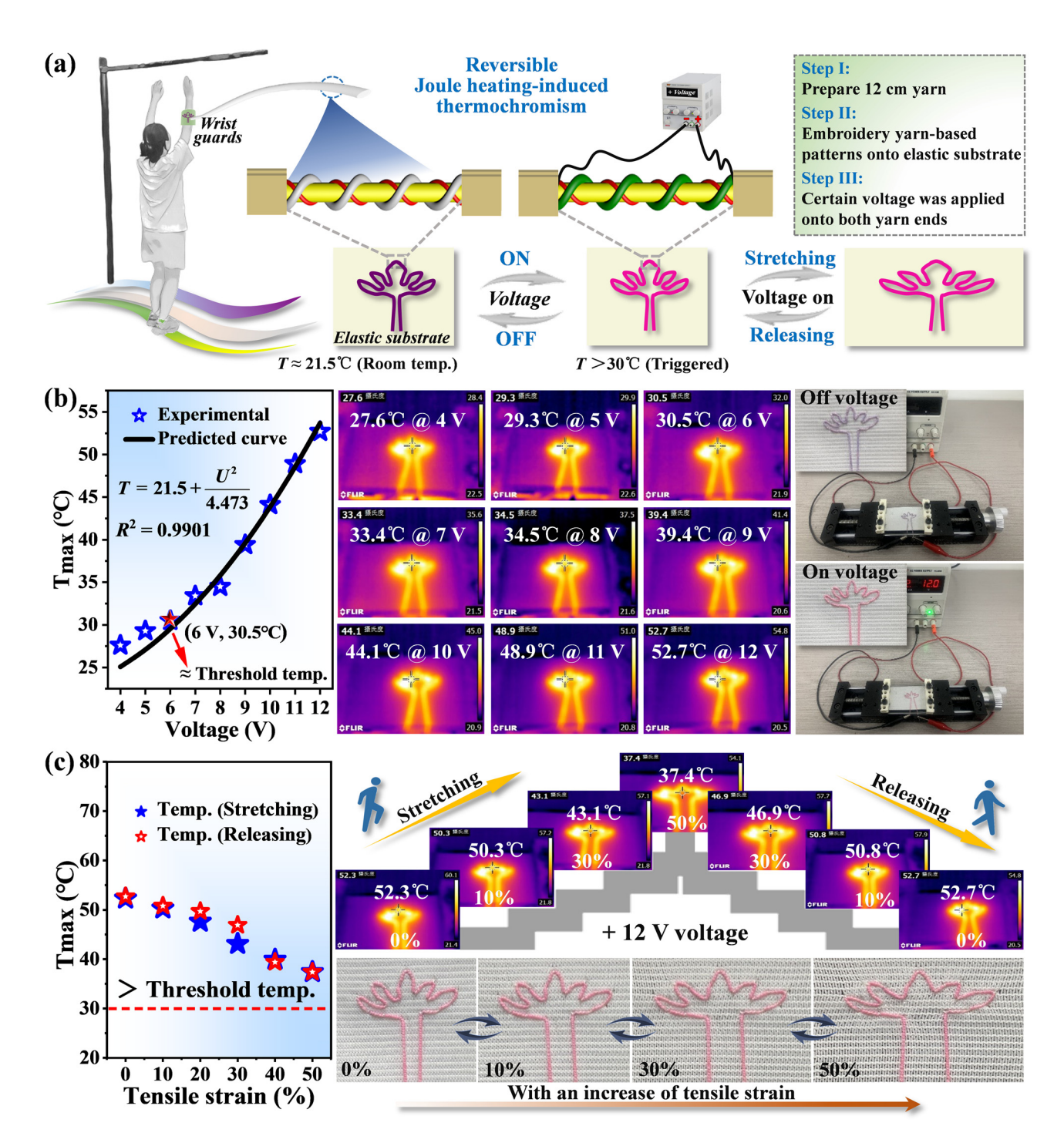


Figure 6: (a) Fabricating elastic flower-shaped pattern as stretchable dynamic colored displays; (b) and (c) thermochromic behavior of such pattern in the initial state and during the stretch, respectively.

to 50% tensile strain. There is a positive relationship between the thermal insulation behavior and the thickness (yarn diameter) (29,30). Thus, the decreased yarn diameter and less still air stored within a yarn during stretch is mainly responsible for the decreased temperature variation trend. Furthermore, there was little hysteresis on

surface temperature when the strain was released, demonstrating the repeatable thermochromic behavior of such a yarn-embroidered pattern. Interestingly, in general, the temperature during the releasing process seems to be slightly higher than that of the temperature during the stretch. The dissipated Joule heat gathering around the

pattern during the stretch is responsible for the enhanced heating during the releasing process. Also, the temperature variation of the pattern during a single stretch-release cycle was also visually reflected in consecutive thermal images. In addition, no obvious variation in color was observed with increasing strains of the pattern (0–50%). The temperature of 37.4°C even if at a larger strain of 50% (still higher than the threshold temperature of 30°C) is mainly responsible for the color retention.

It should be noted that the wrapped yarn-embroidered patterns and the color change can be custom-designed on demand by selecting various thermochromic textile filaments with different color changes or threshold temperatures.

4 Conclusions

In this article, a straightforward and scalable fabrication procedure of highly stretchable thermochromic wrapped yarns with distinctive architecture, which employs EF as core, SSW and TCPF as the first and second helical winding around the EF core, was proposed. The first layer of SSW was used as a heat-conducting material and can generate Joule heat by precisely controlling the voltage, and the thermochromic effect of the second layer of TCPF can be triggered when the heat reaches the threshold temperature. Note that different types of metal wires and metalized yarns could be chosen as heat-conducting materials, in order to optimize the design of yarns.

The effect of elastane draft on the structure and properties of wrapped yarns was clarified. It was found that the elastane draft played an essential role in deciding the stretchability and the final behavior of the resultant yarns, and the optimized elastane draft was obtained at the elastane draft of 2.5 using TOPSIS. It is the spiral geometrical configuration of SSW and TCPF within the yarn and the draw ratio applied to EF that are responsible for the exceptional stretchability of as-prepared yarns. Furthermore, the yarns exhibited super mechanical robustness following cyclic stretch events even at larger tensile strains. More importantly, the yarn exhibited rapid, durable, and reversible color conversion when subjected to cyclic voltage, cyclic abrasion, and alkali. Finally, the wrapped yarn could be easily integrated onto an elastic textile substrate to design desirable patterns using traditional embroidery method, to meet different usage scenarios. As a proof of concept, a flower-shaped pattern was prepared. It was found that the color conversion can be realized when Joule heating-triggered temperature beyond threshold

temperature, and no obvious variation of color fidelity of such pattern was observed under different amounts of stretch. This research work provides some insights toward further advancement of topologically complex, stretchable dynamic colored displays.

Funding information: This research work was financially supported by Open Project of Advanced Fiber Materials Engineering Research Center of Anhui Province (grant number: 2023AFMC14); Open Project of Key Laboratory of Clean Dyeing and Finishing Technology of Zhejiang Province (grant number: QJRZ2115); Open Project of National Local Joint Laboratory for Advanced Textile Processing and Clean Production; Science and Technology Project of Wuhu City (grant number: 2022yf59); National College Student Innovation and Entrepreneurship Training Program (202310363053); Scientific Research Project of Anhui Polytechnic University (grant number: Xjky2022074, FFBK202221, FFBK202336).

Author contributions: Wang Yong: conceptualization, methodology, investigation, writing – original draft, data curation, and funding acquisition. Lizheng Zhang: investigation, writing – original draft. Mingkun Qi: investigation. Zihan Yuan: investigation. Mingwei Li: methodology, supervision. Wei Wang: supervision. Li Changlong: writing – review and editing, supervision. Malik Yonis Hassan Saty: Writing – review and editing, supervision. The authors applied the SDC approach for the sequence of authors.

Conflict of interest: The authors state no conflict of interest.

Data availability statement: The data sets generated during and/or analyzed during the current study are available from the corresponding author on reasonable request.

References

- (1) Meng X, Jia XY, Qi YZ, Miao DG, Yan X. Fabrication of polylactic acid nanofibrous yarns for piezoelectric fabrics. e-Polymers. 2023;23(1):20230030. doi: 10.1515/epoly-2023-0030.
- (2) Zhao HM, Dai Z, He T, Zhu SF, Yan X, Yang JJ. Fabrication of PANI-modified PVDF nanofibrous yarn for PH sensor. e-Polymers. 2021;22(1):69–74. doi: 10.1515/epoly-2022-0013.
- (3) Dai Z, Yan FF, Qin M, Yan X. Fabrication of flexible SiO₂ nanofibrous yarn via a conjugate electrospinning process. e-Polymers. 2020;20(1):600−5. doi: 10.1515/epoly-2020-0063.
- (4) Liang JC, Ding L, Yu ZL, Zhang XC, Chen SG, Wang YF. Smart and programmed thermo-wetting yarns for scalable and customizable moisture/heat conditioning textiles. J Colloid Interf Sci. 2023;651:612–21. doi: 10.1016/j.jcis.2023.08.013.

- (5) Xiong JQ, Chen J, Lee PS. Functional fibers and fabrics for soft robotics, wearables, and human-robot interface. Adv Mater. 2020;33(19):2002640. doi: 10.1002/adma.202002640.
- (6) Shi QW, Sun JQ, Hou CY, Li YG, Zhang QH, Wang HZ. Advanced functional fiber and smart textile. Adv Fiber Mater. 2019;1(1):3–31. doi: 10.1007/s42765-019-0002-z.
- (7) Civan L, Kurama S. A review: Preparation of functionalized materials/smart fabrics that exhibit thermochromic behavior. Mater Sci Tech. 2021;37(18):1405–20. doi: 10.1080/02670836.2021.2015844.
- (8) Duan MH, Wang XC, Xu WX, Ma Y, Yu JY. Electro-thermochromic luminescent fibers controlled by self-crystallinity phase change for advanced smart textiles. ACS Appl Mater Interfaces. 2021;13(48):57943–51. doi: 10.1021/acsami.1c17232.
- (9) Fan HW, Li QL, Li KR, Hou CY, Zhang QH, Li YG, et al. Stretchable electrothermochromic fibers based on hierarchical porous structures with electrically conductive dual-pathways. Sci China Mater. 2020;63(12):2582–9. doi: 10.1007/s40843-020-1404-y.
- (10) Li KR, Zhang QH, Wang HZ, Li YG. Red, green, blue (RGB) electrochromic fibers for the new smart color change fabrics. ACS Appl Mater Interfaces. 2014;6(15):13043–50. doi: 10.1021/am502929p.
- (11) Li YM, Zhang ZT, Li XY, Zhang J, Lou HQ, Shi X, et al. A smart, stretchable resistive heater textile. J Mater Chem C. 2017;5(1):41–6. doi: 10.1039/c6tc04399b.
- (12) Ran JH, Xu R, Xia R, Cheng DS, Yao JB, Bi SG, et al. Carbon nanotube/ polyurethane core-sheath nanocomposite fibers for wearable strain sensors and electro-thermochromic textiles. Smart Mater Struct. 2021;30(7):075022. doi: 10.1088/1361-665X/ac0397.
- (13) Zhang YK, Hu ZX, Xiang HX, Zhai GX, Zhu MF. Fabrication of visual textile temperature indicators based on reversible thermochromic fibers. Dye Pigment. 2019;162:705–11. doi: 10.1016/j.dyepig.2018.11.007.
- (14) Zou XL, Shang SL, Liu J, Ci MY, Zhu P. Facile fabrication of temperature triggered thermochromic core-sheath alginate microfibers from microfluidic spinning. Fiber Polym. 2021;22(6):1535–42. doi: 10.1007/s12221-021-0778-3.
- (15) Galinski H, Leutenegger D, Amberg M, Krogh F, Schnabel V, Heuberger M, et al. Functional coatings on high-performance polymer fibers for smart sensing. Adv Funct Mater. 2020;30(14):1910555. doi: 10.1002/adfm.201910555.
- (16) Sarabia-Riquelme R, Andrews R, Anthony JE, Weisenberger MC. Highly conductive wet-spun PEDOT: PSS fibers for applications in electronic textiles. J Mater Chem C. 2020;8(33):11618–30. doi: 10. 1039/d0tc02558e.
- (17) Li P, Sun ZH, Wang R, Gong YC, Zhou YT, Wang YW, et al. Flexible thermochromic fabrics enabling dynamic colored display. Front Optoelectron. 2022;15(1):40. doi: 10.1007/s12200-022-00042-3.
- (18) Wang Y, Ren J, Ye C, Pei Y, Ling SJ. Thermochromic silks for temperature management and dynamic textile displays. Nano-Micro Lett. 2021;13:72. doi: 10.1007/s40820-021-00591-w.

- (19) Sin D, Singh VK, Bhuyan P, Wei YW, Lee HM, Kim BJ, et al. Ultrastretchable thermo- and mechanochromic fiber with healable metallic conductivity. Adv Electron Mater. 2021;7(8):2100146. doi: 10.1002/aelm.202100146.
- (20) Yang MY, Pan JJ, Luo L, Xu AC, Huang JJ, Xia ZG, et al. CNT/cotton composite yarn for electro-thermochromic textiles. Smart Mater Struct. 2019;28(8):085003. doi: 10.1088/1361-665X/ab21ef.
- (21) Pan JJ, Hao BW, Xu PJ, Li DQ, Luo L, Li JQ, et al. Highly robust and durable core-sheath nanocomposite yarns for electro-thermo-chromic performance application. Chem Eng J. 2020;384:123376. doi: 10.1016/j.cej.2019.123376.
- (22) Stylios GK, Chen MX. The concept of psychotextiles; Interactions between changing patterns and the human visual brain, by a novel composite smart fabric. Materials. 2020;13(3):725. doi: 10.3390/ ma13030725.
- (23) Junge T, Brendgen R, Grassmann C, Weide T, Schwarz-Pfeiffer A. Development and characterization of hybrid, temperature sensing and heating yarns with color change. Sensors. 2023;23(16):7076. doi: 10.3390/s23167076.
- (24) Chen HJ, Huang LH. An investigation of the design potential of thermochromic home textiles used with electric heating techniques. Math Probl Eng. 2015;2015:151573. doi: 10.1155/2015/ 151573.
- (25) Jiang S, Yan WD, Cui C, Wang WJ, Yan JT, Tang H, et al. Bioinspired thermochromic textile based on robust cellulose aerogel fiber for self-adaptive thermal management and dynamic labels. ACS Appl Mater Interfaces. 2023;15(40):47577–90. doi: 10.1021/acsami. 3c11692.
- (26) Chowdhury MA, Butola BS, Joshi M. Application of thermochromic colorants on textiles: temperature dependence of colorimetric properties. Color Technol. 2013;129(3):232–7. doi: 10.1111/cote. 12015
- (27) Staffova M, Kucera F, Tochacek J, Tochacek J, Dzik P, Ondreas F, et al. Insight into color change of reversible thermochromic systems and their incorporation into textile coating. J Appl Polym Sci. 2020;138(4):e49724. doi: 10.1002/app.49724.
- (28) Huang GX, Liu LM, Wang R, Zhang J, Sun XM, Peng HS. Smart color-changing textile with high contrast based on single-sided conductive fabric. J Mater Chem C. 2016;4(32):7589–94. doi: 10.1039/c6tc02051h.
- (29) Wang Y, Gordon S, Yu WD, Wang FM. Structural architecture of wearable materials based on tri-component elastic-conductive composite yarn: toward a Joule heating application. Text Res J. 2019;89(16):3303–11. doi: 10.1177/0040517518811937.
- (30) Wang Y, Yu WD, Gordon S, Wang FM. Parametric study on some physical behaviors of tri-component elastic-conductive composite yarns with different elastane drafts. Text Res J. 2019;89(11):2163–76. doi: 10.1177/0040517518786282.